Limitations of Richardson Extrapolation and Some Possible Remedies

Ismail Celik[1]
Jun Li
Gusheng Hu
Christian Shaffer

Mechanical and Aerospace Engineering Department,
West Virginia University,
Morgantown, WV 26506-6106

The origin of oscillatory convergence in finite difference methods is investigated. Fairly simple implicit schemes are used to solve the steady one-dimensional convection-diffusion equation with variable coefficients, and possible scenarios are shown that exhibit the oscillatory convergence. Also, a manufactured solution to difference equations is formulated that exhibits desired oscillatory behavior in grid convergence, with a varying formal order of accuracy. This model-error equation is used to statistically assess the performance of several methods of extrapolation. Alternative extrapolation schemes, such as the deferred extrapolation to limit technique, to calculate the coefficients in the Taylor series expansion of the error function are also considered. A new method is proposed that is based on the extrapolation of approximate error, and is shown to be a viable alternative to other methods. This paper elucidates the problem of oscillatory convergence, and brings a new perspective to the problem of estimating discretization error by optimizing the information from a minimum number of calculations. [DOI: 10.1115/1.1949646]

1 Introduction

Richardson extrapolation [1,2] is a commonly used method for quantifying the discretization errors in CFD (computational fluid dynamics) applications in fluids engineering and heat transfer problems. In the asymptotic range (i.e., for sufficiently small mesh size h), it is postulated (see Eq. (3.1))

$$\phi - \phi_h = ah^p \tag{1.1}$$

where p is the apparent order of the numerical scheme used, ϕ is the extrapolated solution, and ϕ_h is the numerical solution with mesh size h; a is a coefficient independent of h, but may change in space or time.

Richardson extrapolation uses calculations on multiple sets of grids (see also Sec. 5) to calculate the extrapolated value of a dependent variable to zero grid size, either using the theoretical order of the scheme (on at least two grid levels) or via the apparent or observed order that is calculated as part of the unknowns; in the latter case, at least three sets of calculations are needed on significantly different grid levels. The pros and cons of this method have been the topic of many recent publications [3–10]. In spite of it being a very useful tool for quantifying discretization errors in CFD, there still remain major problems that need to be addressed to advance the level of confidence that could be placed in this method.

This paper addresses the problem of oscillatory convergence. Several questions concerning the oscillatory convergence are (i) Does oscillatory convergence occur? (ii) What happens in the asymptotic range? Asymptotic range means the leading error term dominates in the Taylor expansion of the error function. (iii) Is Richardson extrapolation applicable to oscillatory converging cases? (iv) How can one best make use of results from an oscillatory converging computation?

Answers to the above questions are sought in the following order. First, some examples of oscillatory convergence are presented. Then, the existence of oscillatory is convergence exhibited by constructing (manufacturing) schemes whose discretization errors are forced to satisfy an oscillatory function when applied to a simple convection-diffusion equation. Several modeled equations are given to provide a large number of oscillatory samples. Different, viable methods are evaluated statistically, based on their performance in predicting the exact solution in the limit as h $\rightarrow 0$ using the sample data.

2 Examples of Oscillatory Convergence

We start by giving some examples of oscillatory convergence, one from the solution of simple linear PDE

$$(u\phi)_x = (\Gamma\phi_x)_x + \lambda\phi \tag{2.1}$$

and another from the solution of coupled nonlinear PDEs, namely, Navier-Stokes equations for a fairly complex problem utilizing a readily available commercial code. Here, $()_x$ denotes differentiation with respect to x.

As shown in the Appendix, one example is given by solving a simple steady one-dimensional convection-diffusion equation. The solutions (ϕ) at $x=0.5$ with different grid sizes h are shown in Fig. 1. Oscillatory convergence is seen to occur. The amplitudes of the error change less and less when h approaches zero. In the asymptotic range, as $h \rightarrow 0$ there seems to be at least three terms of the same order of magnitude no matter how small the h value is. More examples are given in the Appendix, where it is shown that oscillatory convergence may also occur with nonmixed schemes, i.e., central differencing.

Another example of oscillatory convergence can be observed in Fig. 2. The solutions were calculated using the FLUENT computational fluid dynamics (CFD) package for two-dimensional turbulent flow past a backward-facing step based on three sets of grids [11]. The expansion ratio is 9/8. The origin (0,0) is located at the lower corner of the step. U is the streamwise velocity, $\Delta U = U - U_{\text{med}}$, where U_{med} is the value calculated on the medium grid. The reference velocity U_{ref} is the maximum streamwise velocity at the inlet. If monotonic convergence happens, the solution with the medium grid should always be in between the solutions given by the coarse grid and the fine grid. However, this is not the case at several points between $y/H=1.5$ and $y/H=3$, where H is the step height.

[1]Please send all communications to the first author at Ismail.Celik@mail.wvu.edu
Contributed by the Fluids Engineering Division for Publication in the JOURNAL OF FLUIDS ENGINEERING. Manuscript received by the Fluids Engineering Division August 27, 2004; Final manuscript received: April 27, 2005; Review conducted by: Subrata Roy.

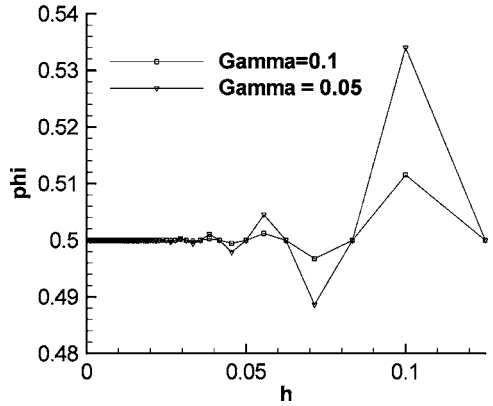

Fig. 1 An example of oscillatory convergence. First-order upwinding scheme applied to the convection term and second-order central differencing applied to the diffusion term with $u=\cos(4\pi x)$; Γ is the diffusion coefficient. (see Appendix)

3 Existence of Oscillatory Convergence

It has been argued [12,13] that oscillatory convergence cannot occur in the asymptotic range. At first glance, this argument seems reasonable in that as $h\to 0$ the leading term in the Taylor series expansion (3.1) dominates

$$\phi(h)=\phi(0)+a_1h+a_2h^2+a_3h^3+\cdots \tag{3.1}$$

where

$$a_k=\frac{1}{k!}\left(\frac{\partial^{(k)}\phi}{\partial h^k}\right)_{h=0} \qquad \mathrm{k}=1,2,3\ldots \tag{3.2}$$

hence, the error $E(h)$ can be expressed as

$$E(h)=\phi(h)-\phi(0)=a_ph^p \tag{3.3}$$

For $p\geqslant 0$, (3.3) shows that E is a monotonic function of h in the asymptotic range. This argument is flawed in the sense that it inherently assumes that the derivatives of $\phi(h)$ and, thus, a_k (3.2) are small as $h\to 0$. This is not necessarily so and it depends on the particular scheme. In fact, for upwind methods, and for mixed methods (i.e., different schemes being activated at different grid levels or in different flow regions), these derivatives are discontinuous. For a consistent scheme (stable and convergent), Eq. (3.3) is not a necessary condition—but a desirable condition.

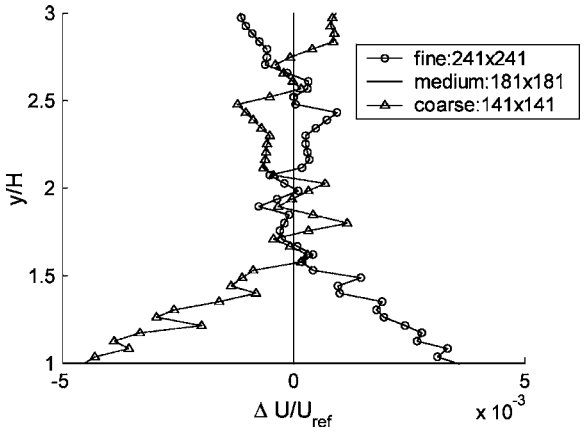

Fig. 2 Normalized streamwise velocity difference based on the medium grid at $x/H=1$ in a 2D turbulent flow over a backward-facing step (using FLUENT and Spalart-Allmaras turbulence model [11])

We can actually construct numerical schemes that force the discretization error to satisfy an oscillatory function. This idea follows a similar line of thinking to manufacture solutions for PDE. Here, we not only manufacture the solution but also derive the corresponding finite difference (FD) scheme. To do this, we use, as an example, a steady convection-diffusion equation with a source term

$$u\phi_x=\phi_{xx}-\lambda\phi \tag{3.4}$$

with boundary conditions $\phi(0)=0$ and $\phi(1)=1$.

Here, ϕ is the exact solution to (3.4), u is the convection velocity, and λ is a constant. The numerical solution $\tilde{\phi}$ with a finite difference scheme on a three-point stencil satisfies a general formula

$$-a_i\tilde{\phi}_{i-1}+b_i\tilde{\phi}_i-c_i\tilde{\phi}_{i+1}=0 \tag{3.5}$$

where a_i, b_i, and c_i are the coefficients of the discretized equation. They must satisfy

$$b_i=a_i+c_i+\lambda \tag{3.6}$$

in order that $\phi=$const is a solution when $\lambda=0$. We further assume that the scheme satisfies an additional condition

$$a_i=c_i+\frac{u_i}{h} \tag{3.7}$$

Let the discretization error E_i satisfy

$$E_i\equiv\tilde{\phi}_i-\phi_i=g_if \tag{3.8}$$

Assume

$$g_i=\beta(i-1)(nx-i) \tag{3.9}$$

$$f=h^p\cos(kh) \tag{3.10}$$

so that the error will be zero at the boundaries and oscillate inside of the domain. nx in (3.9) is the total grid number in the x direction. β is the coefficient that determines the amplitude of the oscillation. Based on the above assumptions, the solution $\tilde{\phi}_i$ is

$$\tilde{\phi}_i=\phi_i+g_ih^p\cos(kh) \tag{3.11}$$

Substituting $\tilde{\phi}$ into Eq. (3.5), we have

$$-a_i(\phi_{i-1}+g_{i-1}f)+b_i(\phi_i+g_if)-c_i(\phi_{i+1}+g_{i+1}f)=0 \tag{3.12}$$

Substituting (3.6) and (3.7) into Eq. (3.12), we obtain the solution

$$b_i=\frac{C-Au_i/h}{A+B} \tag{3.13}$$

where $A=(\phi_i-\phi_{i-1})+(g_i-g_{i-1})f$, $B=(\phi_i-\phi_{i+1})+(g_i-g_{i+1})f$ and $C=-\lambda(\phi_i+g_if)$. a_i and c_i can be solved for by substituting (3.13) back into (3.6) and (3.5). All these coefficients form a new scheme that one may not be familiar with. However, it ensures that the discretization errors oscillate when we refine the grids. In Fig. 3, it is shown that the manufactured scheme from (3.13), (3.6), and (3.7) do indeed result in the oscillatory solutions ϕ_n and exhibit oscillatory convergence as we designed in Eq. (3.8).

4 Modeled Equations for Oscillatory Convergence

Richardson extrapolation is based on the assumption that the first term of the Taylor expansion of the discretization error is dominant. As explained above, when oscillatory convergence occurs, this assumption may not be true, which makes the oscillatory convergence an unresolved problem. In an effort to statistically identify a good method from various possible methods to solve this problem, we need first to have a statistically significant number of oscillatory solution samples. To get these samples, we pro-

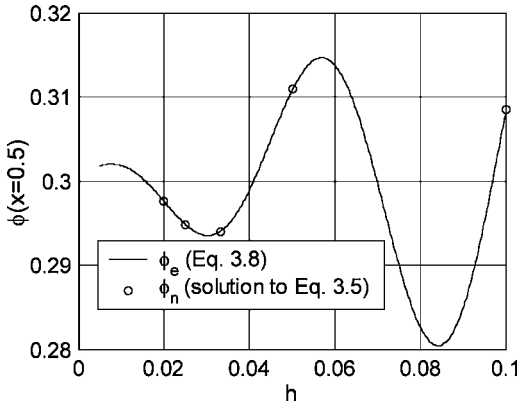

Fig. 3 Designed solutions ϕ_e to Eq. (3.8) and numerical solutions ϕ_n to Eq. (3.5) with the manufactured scheme

pose to use the following oscillatory model equations, which may represent the oscillatory convergence behavior of the solutions to a finite difference equation as shown in Sec. 2 and 3. These models include

$$\phi(h) = \phi_0 + a\cos(2\pi kh)h^p \quad (p \geqslant 1) \tag{4.1}$$

$$\phi(h) = \phi_0 + a(1 - e^{-bh})\cos(2\pi kh)h^p \quad (p \geqslant 0) \tag{4.2}$$

$$\phi(h) = \phi_0 + a\log(1+h)\cos(2\pi kh)h^p \quad (p \geqslant 0) \tag{4.3}$$

These equations can represent the error behavior of any scheme of first order or higher. a, k, and p (or $p+1$) correspond to the maximum error amplitude, the oscillation frequency, and the order of the scheme, respectively. Figure 4 depicts the oscillatory behavior of Eq. (4.1) for various values of k and p. It should be noted here that k, in general, can be a function of h, which means that the oscillation period could be a function of h. However, in the present study, k will be treated as an additional independent parameter. Let the refinement factor be a constant α such that

$$h_i = \alpha^{(i-1)}h_1 \tag{4.4}$$

with $i=1,2,3$ for three sets of grids and $i=1,2,3,4$ for four sets of grids. In the present analysis, α has been assigned the value of $\{0.5, 0.6, 0.7, 0.8, 0.9\}$, which represent the usual ranges in which the grid refinements are done. Without loss of generality, we can normalize h_1 to be 1 (i.e., $h \leftarrow h/h_{\max}$). By changing a, k, and p as listed in Table 1, we have ensembled 270 samples from oscillatory convergence and 270 samples for monotonic convergence. In what follows, we use these samples to assess the performance of various extrapolation methods.

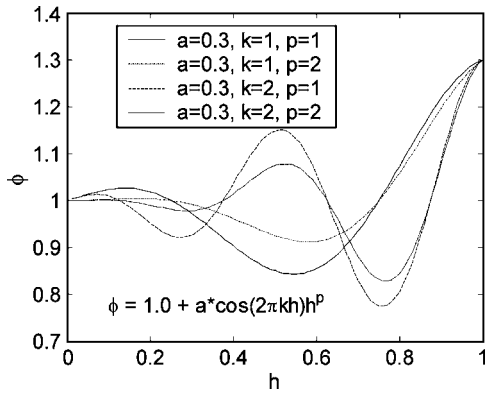

Fig. 4 An example of the behavior of oscillatory model Eq. (4.1)

Table 1 Parameter assignments in Eqs. (4.1)–(4.3)

a	0.2, 0.4, 0.6
k	0.5, 1 (for oscillatory); 0.01, 0.02 (for monotonic)
p	1, 2, 3
b	1
ϕ_0	1.0

5 Methods of Extrapolation for Oscillatory Convergence

In this section, we present the statistical results with four different methods that have the potential to solve the extrapolation problem in oscillatory convergence. These methods include (i) the polynomial method, (ii) the power law method, (iii) the cubic spline method, and (iv) the newly proposed approximate error spline method.

i. Polynomial method. This method uses the first few terms in Eq (3.1) to approximate $\phi(0)$. For instance, assuming the method is first order, we can use the first three terms if we have three sets of grids. That is,

$$\phi(h) = \phi(0) + a_1 h + a_2 h^2 \tag{5.1}$$

If we have four sets of grids, then we can use

$$\phi(h) = \phi(0) + a_1 h + a_2 h^2 + a_3 h^3 \tag{5.2}$$

If the discretization scheme has an order of two or higher, this method means essentially a curve fit to the actual error function. For a fourth-order method, one has to keep at least four terms, i.e., five sets of calculations are needed.

The extrapolation to the limit approach [14,15] is recommended to solve the equations formed by the polynomial method. This approach uses the following formula to calculate the extrapolated solution $\phi^{(3)}(h)$ for three sets of grids and $\phi^{(4)}(h)$ for four sets of grids:

$$\phi^{(m)}(h) = \frac{\phi^{(m-1)}(\alpha h) - \alpha^m \phi^{(m-1)}(h)}{1 - \alpha^m} \quad \mathrm{m} = 1,2,\ldots \tag{5.3}$$

It is easy to tabulate the sequential steps of the calculation procedure and to add more points later.

ii. Power law method. We use the power law method proposed by Celik and Karatekin [7] for three sets of grids. The idea follows:

$$\phi(0) - \phi(h_1) = ch_1^p \tag{5.4}$$

$$\phi(0) - \phi(h_2) = \mathrm{sign}\left(\frac{\varepsilon_{32}}{\varepsilon_{21}}\right)ch_2^p \tag{5.5}$$

$$\phi(0) - \phi(h_3) = ch_3^p \tag{5.6}$$

where $\varepsilon_{32}/\varepsilon_{32} = [\phi(h_3) - \phi(h_2)]/(\phi(h_2) - \phi(h_1))$, the sign of which is positive for monotonic convergence and negative for oscillatory convergence. There are three unknows, $\phi(0)$, c, and p. We can implement the same iterative method to solve (5.4)–(5.6) as done by Celik and Karatekin [7].

For four sets of grids, we can apply

$$\phi(h_i) - \phi(0) = a_1 h_i^p + a_2 h_i^{p+1} \quad i = 1,2,3,4 \tag{5.7}$$

Oscillatory convergence is facilitated if a_1 and a_2 are of opposite sign. It should be noted that for some cases there is no solution to Eq. (5.7). Those cases will be counted as unsuccessful outcomes.

iii. Cubic spline method. The well-known natural cubic splines curve fitting technique is used to create the cubic splines between three points or four points. $\phi(0)$ can be found by extrapolating the curve for the interval closest to $h=0$.

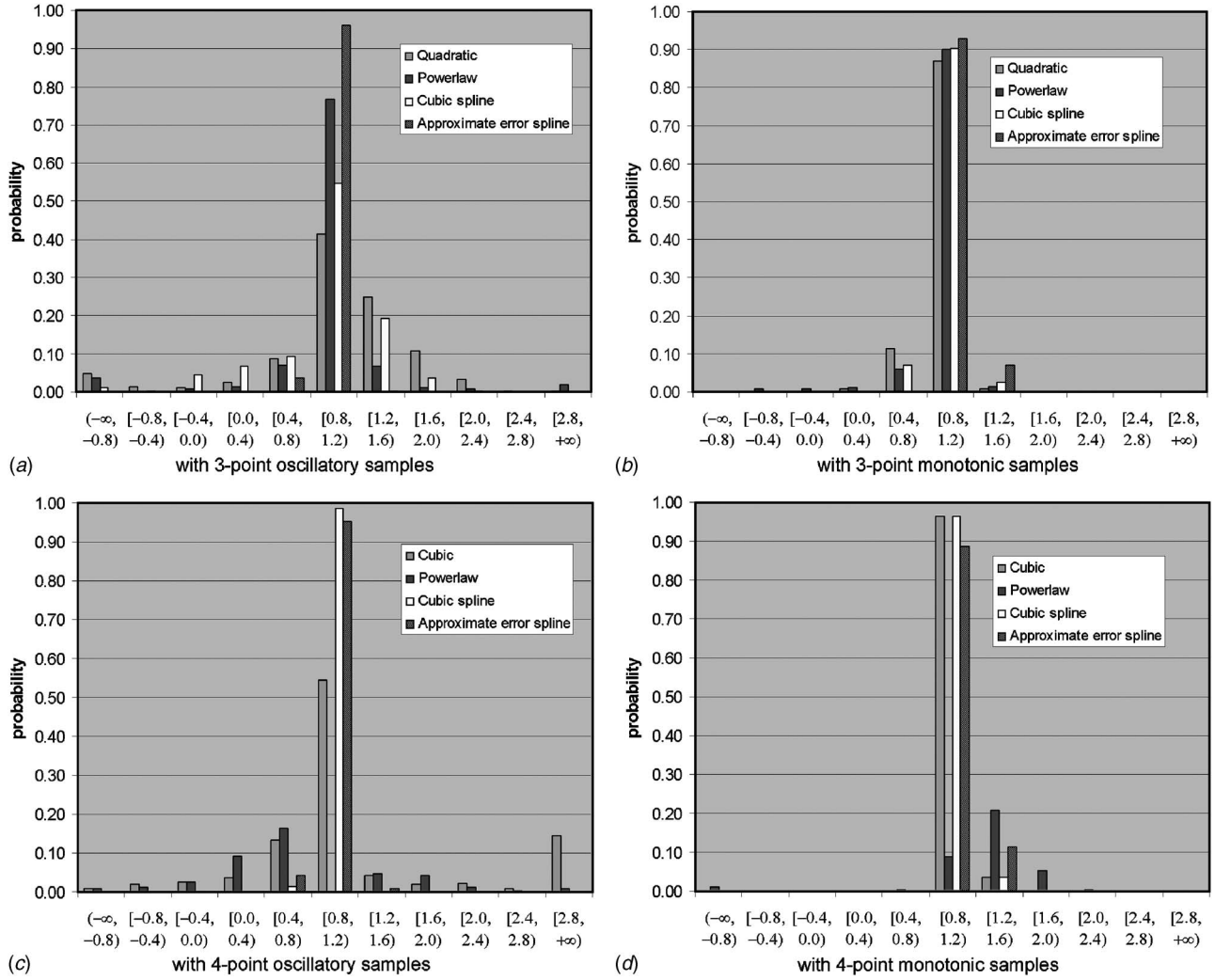

Fig. 5 Probability of $\phi(0)$ at different intervals, predicted with different methods

iv. Approximate error spline methods. Still using Taylor series expansion as in Eq. (3.1) for $\phi(h)$ and substituting αh for h, we have

$$\phi(\alpha h) = \phi(0) + a_1 \alpha h + a_2 (\alpha h)^2 + a_3 (\alpha h)^3 + \cdots \tag{5.8}$$

The true error E_t is given by

$$E_t(\alpha, h) \equiv \phi(\alpha h) - \phi(0) = \sum_{k=1}^{\infty} a_k \alpha^k h^k \tag{5.9}$$

and the approximate error E_a

$$E_a(\alpha, h) \equiv \phi(\alpha h) - \phi(h) \tag{5.10}$$

which presents the difference of the subsequent results with the fine grid and the coarse grid. Subtracting (3.1) from (5.8) gives

$$E_a(\alpha, h) = \sum_{k=1}^{\infty} a_k (\alpha^k - 1) h^k \tag{5.11}$$

Dividing (5.9) by (5.11) and moving $E_a(\alpha, h)$ to the right-hand side yields

Table 2 Probability and norm with different methods for oscillatory and monotonic samples

			Polynomial	Powerlaw	Cubic spline	Approximate error spline
3 points	Oscillatory	Probability in [0.8, 1.2)	41%	77%	55%	96%
		Norm	15.3	25.2	8.10	1.38
	Monotonic	Probability in [0.8, 1.2)	87%	90%	90%	93%
		Norm	2.62	3.55	2.01	1.69
4 points	Oscillatory	Probability in [0.8, 1.2)	54%	0%	99%	95%
		Norm	37.2	112	0.85	1.48
	Monotonic	Probability in [0.8, 1.2)	96%	9%	96%	89%
		Norm	1.43	353	1.27	2.20

Table 3 Probability and norm of extrapolation calculated with the three points out of four points, excluding the coarsest one

		Polynomial	Powerlaw	Cubic spline	Approximate error spline
Oscillatory	Probability in [0.8, 1.2)	67%	88%	73%	99%
	Norm	7.50	8.77	5.98	0.94
Monotonic	Probability in [0.8, 1.2)	95%	94%	96%	92%
	Norm	1.44	5.01	1.36	1.81

$$E_t(\alpha,h)=\frac{1}{1-\dfrac{\sum a_k h^k}{\sum a_k \alpha^k h^k}}E_a(\alpha,h) \tag{5.12}$$

letting

$$\frac{\sum a_k h^k}{\sum a_k \alpha^k h^k}=b_0+b_1 h+b_2 h^2 \tag{5.13}$$

and expanding the left-hand side of the above equation and comparing it with the right-hand side gives

$$b_0=\frac{1}{\alpha}\quad b_1=\left(\frac{1-\alpha}{\alpha}\right)\frac{a_2}{a_1}$$

$$b_2=\left(\frac{1-\alpha^2}{\alpha}\right)\frac{a_3}{a_1}-(1-\alpha)\left(\frac{a_2}{a_1}\right)^2 \tag{5.14}$$

Now Eq. (5.12) can be rewritten as

$$E_t(\alpha,h)=\frac{1}{1-(b_0+b_1 h+b_2 h^2)}E_a(\alpha,h) \tag{5.15}$$

In order to calculate b_0, b_1, and b_2, we need to calculate a_1, a_2, and a_3 first. It is seen from Eq. (5.11) that

$$a_k=\frac{E_a^{(k)}(\alpha,0)}{k\,!\,(\alpha^k-1)}\quad k=1,2,3 \tag{5.16}$$

$E^{(k)}$ is the kth derivative of E. Assuming that we have three sets of grids and the solutions as $[h_1,\phi(h_1)]$, $[h_2,\phi(h_2)]$, and $[h_3,\phi(h_3)]$ with $h_3=\alpha h_2=\alpha^2 h_1$, and noting that $E_a(\alpha,0)\equiv 0$ leads to three points as $[h_1,E_a(\alpha,h_1)]$, $[h_2,E_a(\alpha,h_2)]$, and $[0,E_a(\alpha,0)]$, which involves the approximate error instead of the numerical solution $\tilde{\phi}$ itself. Using the information on E_a, we can interpolate with cubic splines with the endslopes given by $E_a'(\alpha,0)\cong 0$ and $E_a'(\alpha,h_1)\cong[E_a(\alpha,h_1)-E_a(\alpha,h_2)]/(h_1-h_2)$. These endslopes are acceptable at $h=0$ for any scheme with order larger than 1. For the first-order methods, in general, the slope at $h=0$ is not zero. We could still obtain excellent results using the zero slope assumption for the first-order methods, as we demonstrate in the assessment part of this paper. Once we have $E_a^{(k)}(\alpha,0)$, we can calculate a_k from Eq. (5.16). As one might note, b_1 is singular at $h=0$ if $E_a'(\alpha,0)=0$. In order to avoid this singularity, $E_a'(\alpha,\varepsilon)$ can be used to represent $E_a'(\alpha,0)$ by using finite differencing at $h=\varepsilon$, where ε is a small value. Having obtained b_0, b_1, and b_2, we can calculate $\phi(0)$ from Eq. (5.15), together with the definition (5.9) and (5.10).

6 Assessment of Methods

Two parameters are used to evaluate the performance of these methods. One is the case percentage out of 270 samples for which the calculated $\phi(0)$ is in the region of $\phi_0\pm\mu$; with $\mu=0.2$, this represents the confidence level for the interval of ±20% error. Another is the L^2 norm of the true error. Here, the L^2 norm is defined by $L^2=(\Sigma_{\text{cases}}[\phi_0-\phi(0)]^2)^{1/2}$.

Figure 5 shows the probability distribution of the predicted $\phi(0)$ at different intervals with different methods. The probability for $\phi(0)\in[0.8,1.2]$ and the L^2 norm are listed in Table 2. For monotonically converging cases, all methods perform well, with the approximate error spline (AES) method being the best. With three-point oscillatory samples, the approximate error spline method is overwhelmingly superior to the others, and the power law method ranks second best. However, with four-point oscillatory samples, the power law method performs the worst because there are no solutions for 59% of the samples. The cubic spline method and the AES method both perform very well. With three-point monotonic samples, all methods perform well, but the power law method is not applicable for four-point monotonic samples since it's not solvable for 63% of the samples.

However, we can use three solutions on the finer meshes to predict $\phi(0)$ when four solutions are available [13]. For instance, if $[h_1,\phi(h_1)]$, $[h_2,\phi(h_2)]$, $[h_3,\phi(h_3)]$, and $[h_4,\phi(h_4)]$ are available and h_1 is the coarsest grid size, we may use the last three points to calculate $\phi(0)$, and the first three points to confirm the estimation. The results following this thought are shown in Table 3. It should be first noted that the extrapolation based on the coarse three points is the same as shown in the three-point rows of Table 2. It is seen that the extrapolations with the fine three points are better than the ones with the coarse three points. Improvements are also observed in the polynomial, power law, and AES methods when we compare them to the extrapolations with all four points. Out of the four sets of grids, four triplets can be used. The first three and the last three are used separately, and it was found that the last three triplets gave slightly better results than the first three, as should be expected. The other triplets, namely, (1,3,4) and (1,2,4), can be used to confirm the analysis based on the other triplets. This is not done here because the AES method is formulated only for a constant grid refinement ratio. The surprisingly good performance of the AES method can be attributed to the use of the extra information that both E_a and E_t tend to zero as h goes to zero.

7 Conclusions

The origin of oscillatory convergence in finite difference (FD) or finite volume (FV) solutions is investigated. It has been shown that this behavior may occur not only when mixed order methods are used, but also when the coefficients of the FD equations exhibit highly oscillatory behavior. A usual source for such variations could be the oscillatory velocity field that occurs in recirculation regions near separation and reattachment points. By way of manufactured solution to FD equations and constructing a corresponding finite difference scheme, it is shown that there exist infinitely many finite difference methods that will exhibit oscillatory convergence, even in the asymptotic range. This information is then used to construct model error equations that are used to ensemble a large number of cases with oscillatory convergence. These samples are then used to assess the performance of various extrapolation methods for both monotonic and oscillatory cases. The results show that for three-grid calculations, the newly proposed approximate error spline (AES) method performs overwhelmingly superior to the others, the commonly used power law method ranking second best.

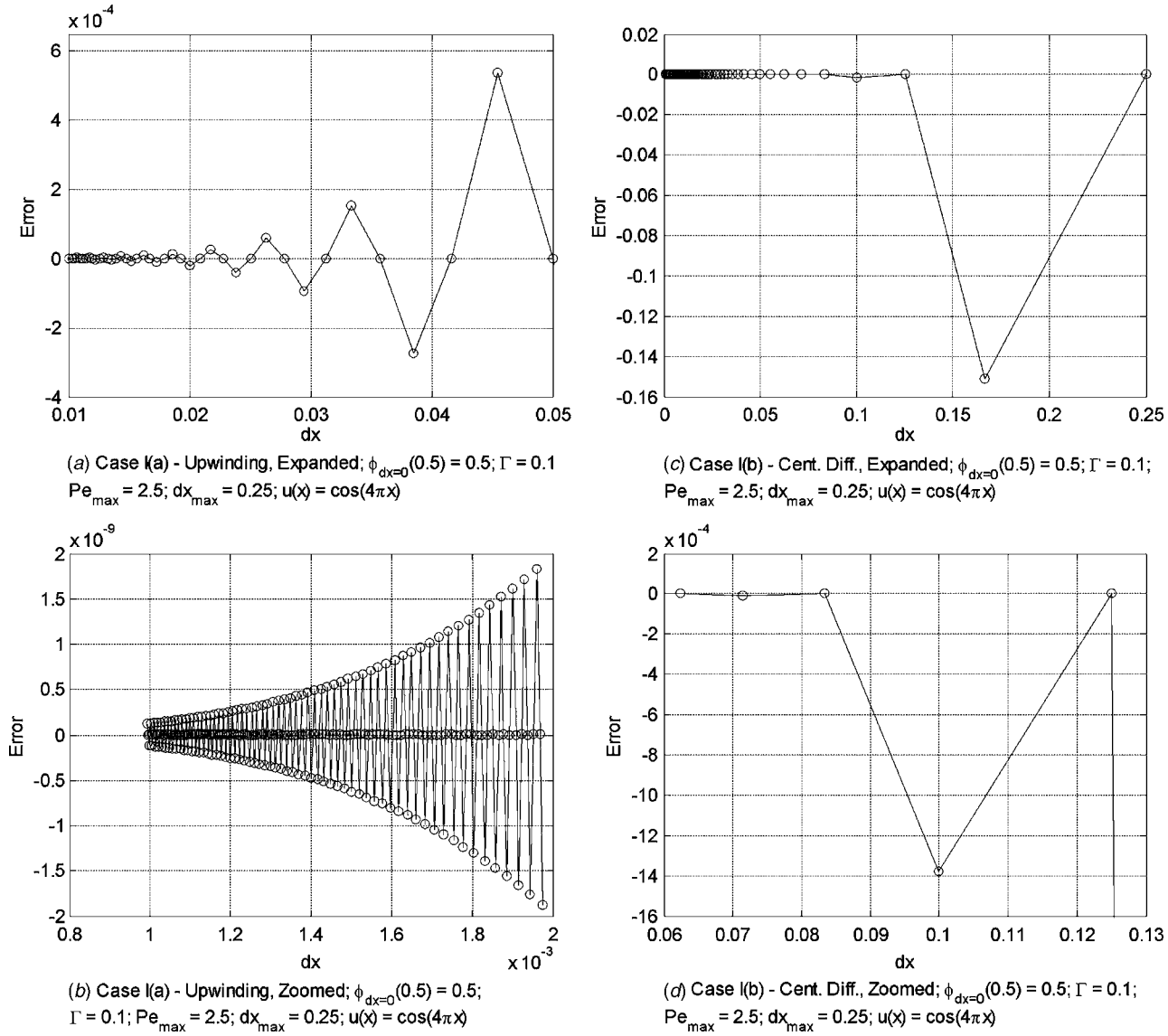

Fig. 6 Error plots showing cases I(a) and I(b) in both expanded and zoomed form

We recommend that four sets of calculations be performed; the last three should be used for extrapolation and the other triplets should be used for confirmation of analysis. When this is done, the best method is the approximate error spline method, and the next best is the power law method for oscillatory convergent cases. For monotonic convergence, all methods perform well.

Nomenclature

a_i, b_i, c_i = coefficients of the discretized equation
a, b, c, a_p, a_k = coefficients
A, B, C = intermediate variables
E_a = approximate error
E_t = true error
f = function of h
g = function of x
h = grid size
p = exponent
Pe = Peclet number
u = convection coefficient
U = velocity component
α = refinement factor
λ = factor
ϕ = variable to be solved
ϕ_n = numerical solution with mesh size h
Γ = diffusion coefficient
Ψ = function of x
ε_{21} = $\phi(h_2) - \phi(h_1)$
ε_{32} = $\phi(h_3) - \phi(h_2)$
ε = a small value
μ = confidence level

APPENDIX: GRID CONVERGENCE TRENDS FOR SOME FINITE DIFFERENCE SCHEMES

In applications of CFD, it is not unusual to observe oscillatory convergence in field variables, such as velocity [11,7]. It is suspected that this behavior is usually a consequence of the use of mixed-order methods such as first-order upwinding mixed with second-order upwinding, or first-order upwinding with central differencing, etc. Here, we investigate the grid convergence behavior of several schemes applied to the steady linear convection diffusion equation with variable velocities $u(x)$ and diffusivity $\Gamma(x)$. The model equations we use are

Conservative form:

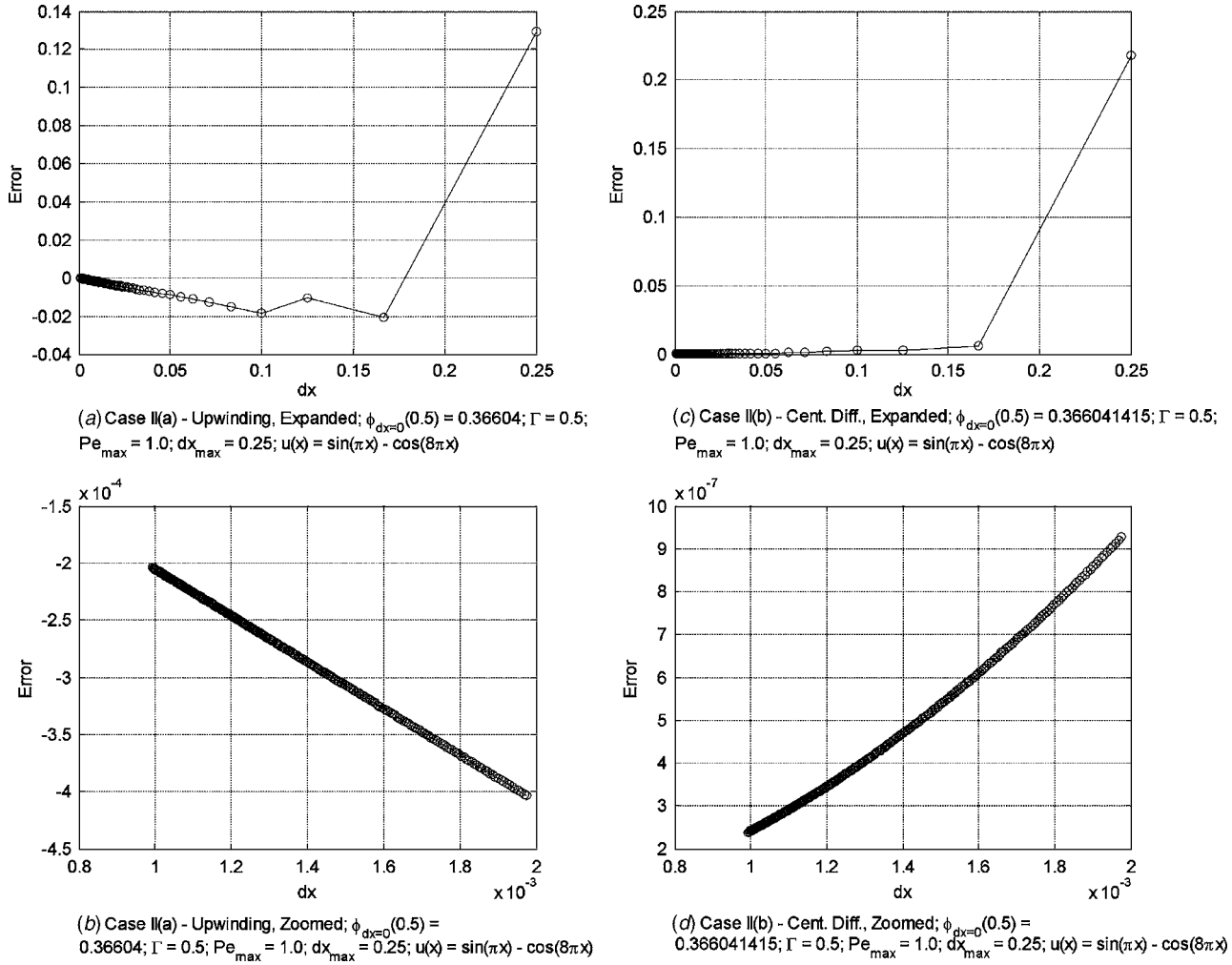

Fig. 7 Error plots showing cases II(a) and II(b) in both expanded and zoomed form; the lower plots show convergence behavior for very small *dx* values

$$\frac{\partial(u\phi)}{\partial x} = \frac{\partial}{\partial x}\left[\Gamma\frac{\partial\phi}{\partial x}\right] + \lambda\phi \tag{A1a}$$

Nonconservative form:

$$u\frac{\partial\phi}{\partial x} = \Gamma\frac{\partial^2\phi}{\partial x^2} + \lambda\phi \tag{A1b}$$

In this study, three different functions were utilized for the fluid velocity given by

$$u(x) = \cos(4\pi x) \tag{A2a}$$

$$u(x) = \sin(\pi x) - \cos(8\pi x) \tag{A2b}$$

$$u(x) = \sin(2\pi x) - \cos(4\pi x) \tag{A2c}$$

In all cases, the boundary conditions used were $\phi(0)=0$ and $\phi(1)=1$. Three different schemes were used in solving this equation: a first-order upwinding scheme, a second-order central differencing scheme, and a hybrid scheme that combined these two schemes based on the cell Peclet number defined as

$$\mathrm{Pe} = \frac{udx}{\Gamma} \tag{A3}$$

When the Peclet number was less than two, the hybrid scheme used the central differencing scheme, and when the Peclet number was greater than two, the hybrid scheme used the upwinding scheme.

In order to avoid using upwinding for the convective term, an alternative semianalytical formulation was also used. In this it was assumed that

$$\phi(x) = f(x)\psi(x) \tag{A4}$$

Substituting (A4) into (A1*a*), with Γ being constant, yields

$$[pf - 2f']\psi' = f\psi'' + [f'' - (pf)']\psi \tag{A5}$$

where $p=u(x)/\Gamma$. Equating the bracketed term on the left-hand side to zero eliminates the first derivative

$$pf - 2f' = 0 \tag{A6}$$

and solving (A6) gives

$$f(x) = e^{(1/2)\int p(x)dx} \tag{A7}$$

Substituting (A7) and its respective derivatives along with (A6) into (A5), after some simplification, we obtain

$$\psi'' = \tfrac{1}{2}\left[p' - \tfrac{1}{2}p^2\right]\psi \tag{A8}$$

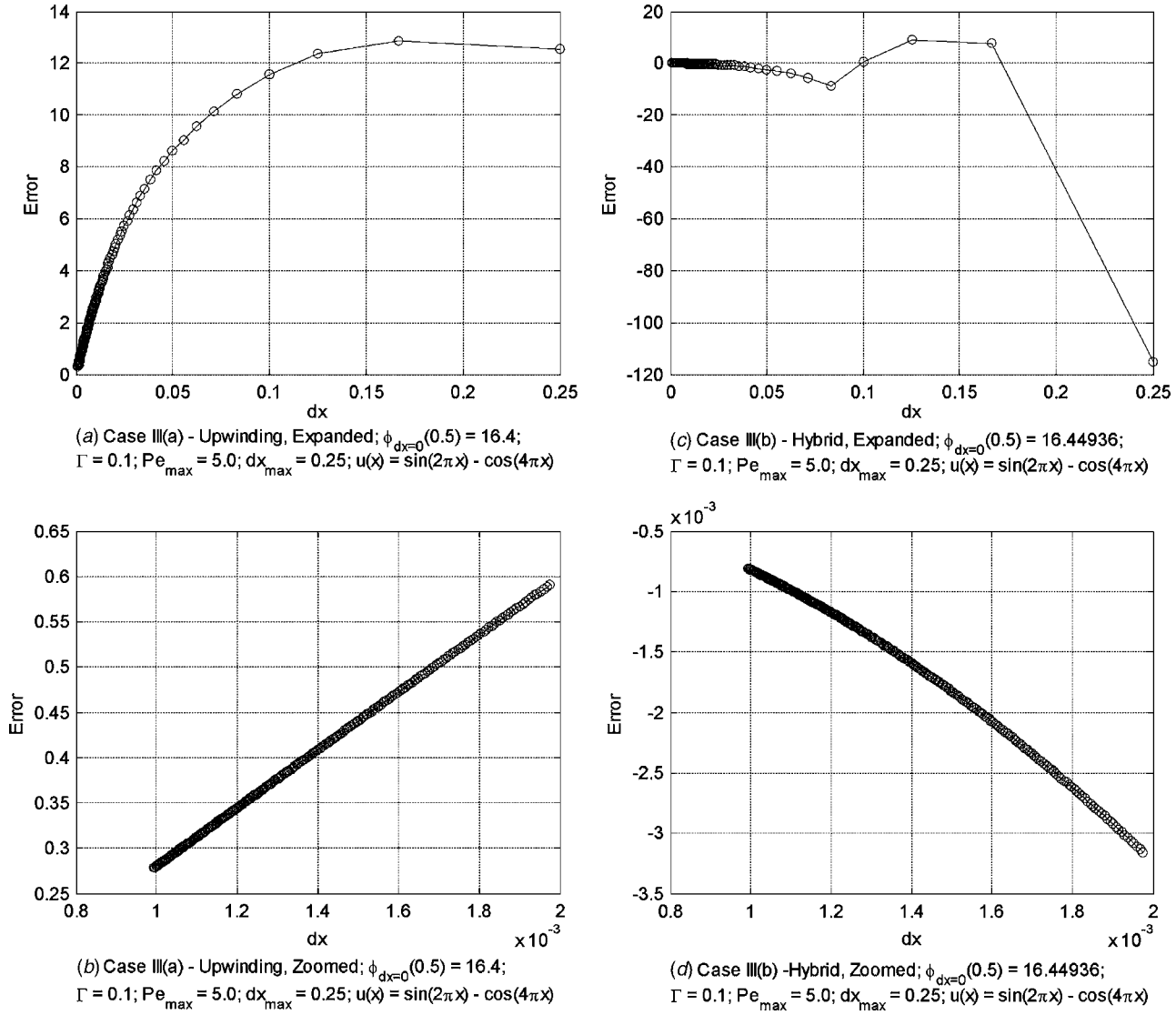

Fig. 8 Error plots showing cases III(a) and III(b) in both expanded and zoomed form; the lower plots show convergence behavior for very small *dx* values

The boundary conditions for (A8) can be derived using relation (A4). Without loss of generality, we can select $f(0)=1.0$ and $f(1.0)=1.0$, hence

$$\psi(0) = 0 \tag{A9a}$$

$$\psi(1) = 1 \tag{A9b}$$

If Eq. (A7) is analytically integrable, this approach avoids the necessity to use upwinding for the convection terms. Equation (A8) can be solved using central differencing for all Peclet numbers.

Exact Solution Verification

As another way of confirming the results from the central differencing and upwinding schemes, the Euler-Cauchy equation was put into the same form as the convection diffusion equation (A1*b*)

$$(x-2)^2\phi'' + 5(x-2)\phi' + 3\phi = 0 \tag{A10a}$$

$$u(x)\phi' = \Gamma(x)\phi'' + 3\phi \tag{A10b}$$

where $u(x)=-5(x-2)$, $\Gamma(x)=(x-2)^2$, and $\lambda=3$ as per Eq. (A1*b*). The analytical solution to this equation was found to be

$$\phi(x) = C_1(x-2)^{-3} + C_2(x-2)^{-1} \tag{A11a}$$

and after applying the boundary conditions $\phi(0)=0$ and $\phi(1)=1$ and solving for constants C_1 and C_2, Eq. (A11*a*) became

$$\phi(x) = \frac{-4}{3(x-2)^3} + \frac{1}{3(x-2)} \tag{A11b}$$

Equation (A11*b*) then gave an analytical solution with which to verify the results from the numerical procedure.

In a final attempt to verify the results of the numerical solutions, a manufactured solution for the steady convection diffusion Eq. (A1*a*) was found. With no source term and additional $f(x)$ terms, Eq. (A1*a*) becomes

$$\frac{\partial(u\phi)}{\partial x} = \frac{\partial}{\partial x}\left[\Gamma\frac{\partial\phi}{\partial x}\right] + f(x) \tag{A12}$$

Assuming a convenient solution $\phi(x)$, a velocity function $u(x)$, and a diffusivity $\Gamma(x)$, $f(x)$ can be determined from

$$f(x) = u\frac{\partial\phi}{\partial x} + \phi\frac{\partial u}{\partial x} - \Gamma\frac{\partial^2\phi}{\partial x^2} - \frac{\partial\phi}{\partial x}\frac{\partial\Gamma}{\partial x} \tag{A13}$$

Next, a two-parameter solution can be assumed

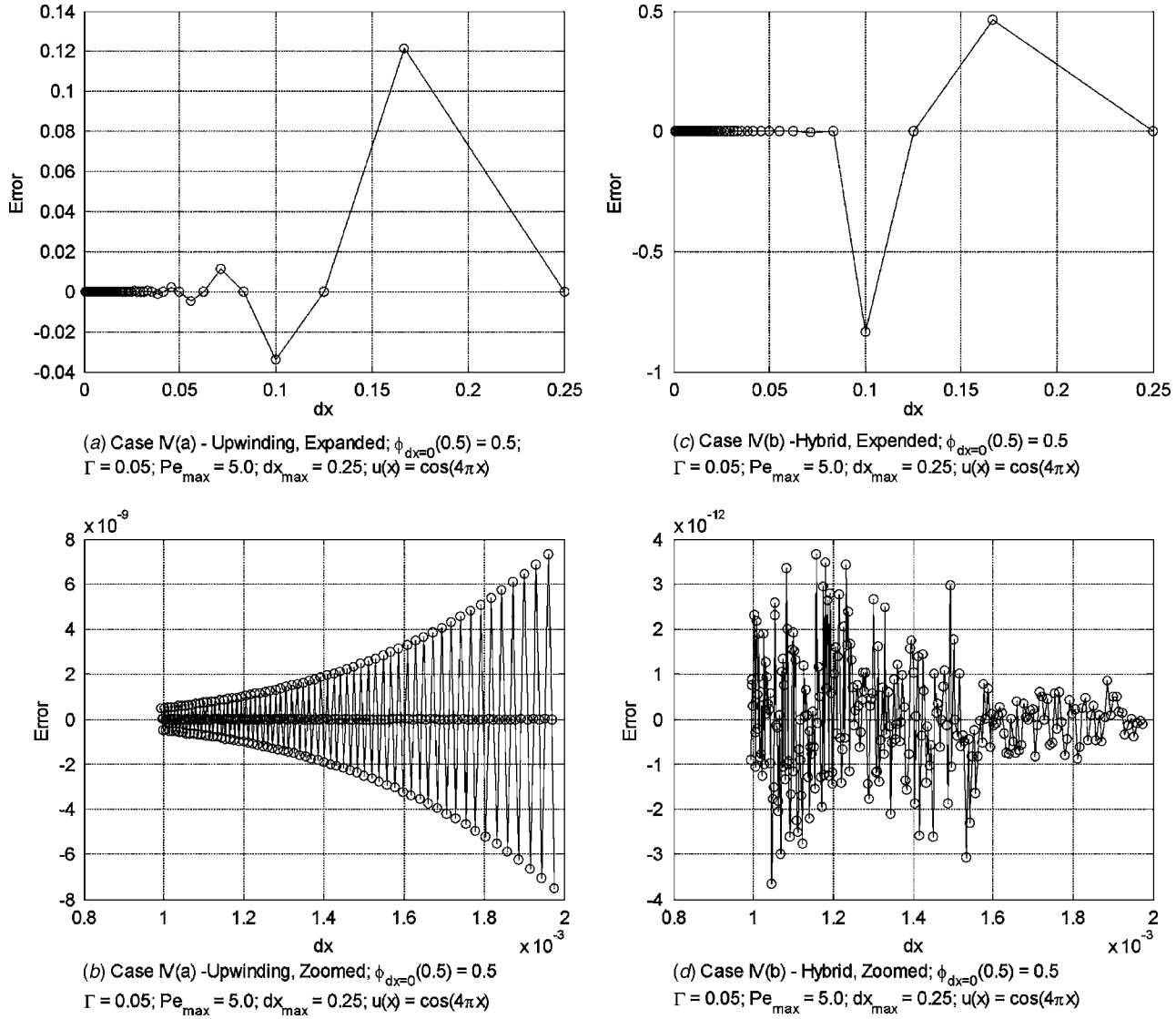

Fig. 9 Error plots showing cases IV(a) and IV(b) in both expanded and zoomed form; the lower plots show convergence behavior for very small dx values

$$\phi(x) = \phi_0 + bx + \tfrac{1}{2}\{\tanh[a(x - x_0)] - c\} \qquad \text{(A14}a\text{)}$$

for $0 \leqslant x \leqslant 1$, with

$$c = \tanh(-ax_0) \qquad \text{(A14}b\text{)}$$

$$b = \phi(1) - \phi(0) - \frac{1}{2}\{\tanh[a(1 - x_0)] - c\} \qquad \text{(A14}c\text{)}$$

where the derivatives of (A14a) are given by

$$\frac{\partial \phi}{\partial x} = b + \frac{a}{2}\{1 - \tanh^2[a(x - x_0)]\} \qquad \text{(A15)}$$

and

$$\frac{\partial^2 \phi}{\partial x^2} = -a^2[\{\tanh[a(x - x_0)]\}][1 - \tanh^2[a(x - x_0)]\}] \qquad \text{(A16)}$$

After calculating $\frac{\partial \phi}{\partial x}, \frac{\partial^2 \phi}{\partial x^2}, u, \frac{\partial u}{\partial x}, \Gamma$, and $\frac{\partial \Gamma}{\partial x}, f(x)$ can be determined from Eq. (A13). A much simpler solution is given by

$$\phi(x) = c(1 - e^{-x}) \qquad \text{(A17)}$$

where $c = (1 - e^{-1})^{-1}$. Letting

$$\Gamma = 0 \qquad \text{(A18)}$$

and

$$u(x) = x(1 - x) \qquad \text{(A19)}$$

it can be deduced from Eq. (A13) that

$$f(x) = \frac{\partial (u\phi)}{\partial x} = x(1 - x)ce^{-x} + c(1 - e^{-x})(1 - 2x) \qquad \text{(A20)}$$

Substituting Eqs. (A18)–(A20) into Eq. (A12), a numerical result is obtained. This result is then compared with the analytical solution given by equation (A17).

Results

A summary of all the cases used is listed in Table 4. This table includes the case number, scheme, velocity function ($u(x)$), diffusivity constant (Γ), and extrapolated solution for each case. Table 4 also shows L^2 error norms for each case with respect to the semianalytical solution for that case. The L^2 error norms show that the numeric solutions seem to be good. These cases will be referred to by their respective case numbers.

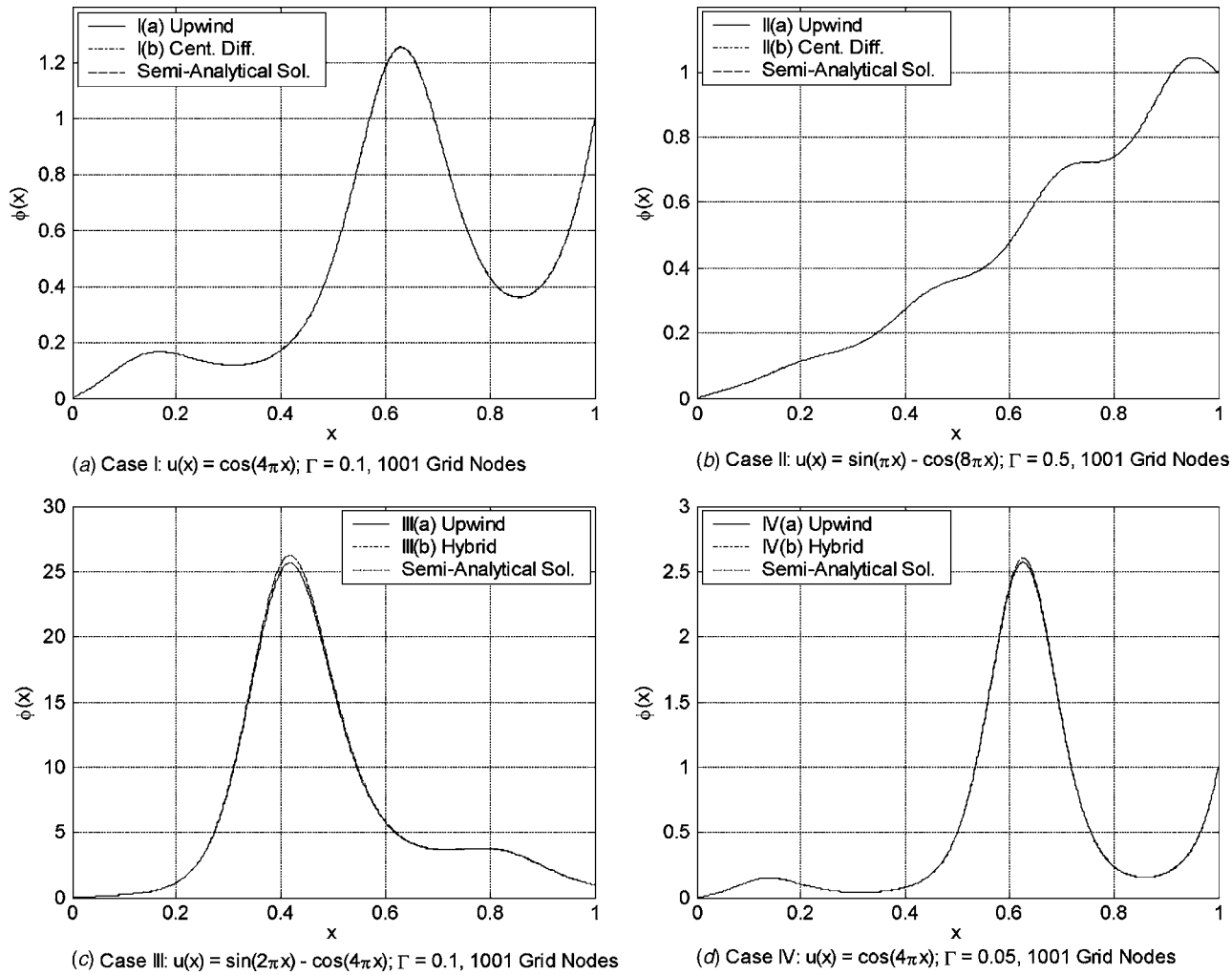

Fig. 10 Solutions for cases I—IV using upwinding and central differencing schemes, as well as the semi-analytical solution

Figures 6–9 show the error using the upwinding, central differencing, and hybrid schemes calculated at $x=0.5$ versus the grid spacing dx. The error is calculated from

$$E_h = \phi_{\text{ext}} - \phi_h(0.5)$$

where $\phi_h(0.5)$ is the solution from the scheme for the respective grid spacing of $h=dx$, and ϕ_{ext} is the extrapolated solution. The extrapolated solutions were found by taking the grid spacing to an appropriately small value and extrapolating with the same trend to $dx=0$. The error bounds for the extrapolated solutions were taken as the difference between the extrapolated solution and the solution at the finest grid spacing used.

Figure 6 shows the error versus the grid spacing for cases I(a) (upwinding) and I(b) (central differencing). Figures 6(*a*) and 6(*b*) show that the convergence with the upwind scheme was oscillatory, even as the grid spacing became very small. In these two plots, the error oscillated cyclically above and below zero as the grid spacing approached zero. Figures 6(*c*) and 6(*d*) show the convergence pattern with the central differencing scheme. With this scheme, the convergence behavior was also oscillatory, but the error oscillated only below zero rather than above and below the zero. Figure 6(*d*) illustrates the fact that even though the central differencing scheme converges very quickly, it still has small oscillations as the grid spacing becomes smaller.

Table 4 Case summary

Case	Scheme	u(x)	Γ	Extrapolated solution at $x=0.5$	L^2 error norm
I(a)	Upwind	$\cos(4\pi x)$	0.1	$0.5+/-0.25\times10^{-10}$	0.9375412
I(b)	Central	$\cos(4\pi x)$	0.1	$0.5+/-0.8\times10^{-11}$	0.0101842
II(a)	Upwind	$\sin(\pi x)-\cos(8\pi x)$	0.5	$0.36604+/-7\times10^{-5}$	0.1139626
II(b)	Central	$\sin(\pi x)-\cos(8\pi x)$	0.5	$0.366041415+/-3\times10^{-8}$	0.0009532
III(a)	Upwind	$\sin(2\pi x)-\cos(4\pi x)$	0.1	$16.4+/-0.12$	122.4437985
III(b)	Hybrid	$\sin(2\pi x)-\cos(4\pi x)$	0.1	$16.44936+/-1\times10^{-4}$	1.1804976
IV(a)	Upwind	$\cos(4\pi x)$	0.05	$0.5+/-1.0\times10^{-10}$	4.8115126
IV(b)	Hybrid	$\cos(4\pi x)$	0.05	$0.5+/-1.0\times10^{-11}$	0.1255890

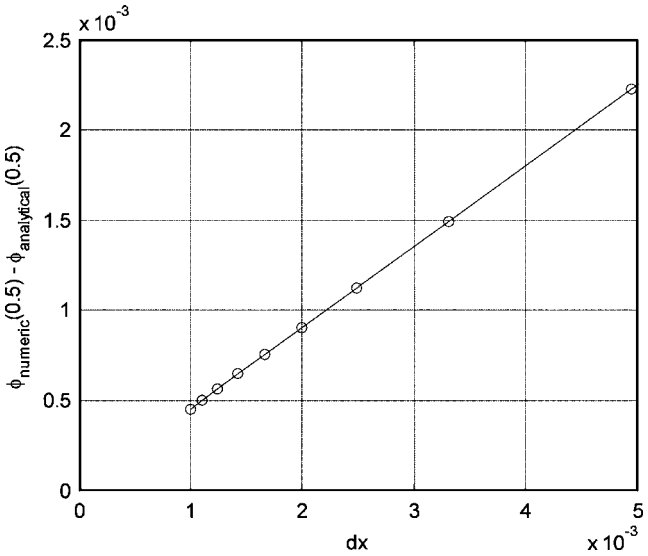

Fig. 11 Difference between analytical and numerical solutions at $x=0.5$ for equation (A10*b*)

Figure 7 gives the error versus the grid spacing for cases II(a) and II(b). Figures 7(*a*) and 7(*b*) illustrate the convergence pattern using an upwind scheme, while Figures 7(*c*) and 7(*d*) show the convergence using the central differencing scheme. It is evident that in both cases as the grid spacing became increasingly small, the solution monotonically approached the extrapolated solution given in Table 4.

For cases III(a) and III(b), Fig. 8 shows the error versus the grid spacing. The convergence pattern using an upwinding scheme is illustrated in Figs. 8(*a*) and 8(*b*), while Figs. 8(*c*) and 8(*d*) show the convergence using the hybrid scheme. Much like the results from cases II(a) and II(b) illustrated in Fig. 7 and 8 shows that once again as the grid spacing became small, the solution monotonically approached the extrapolated solution.

Figure 9 illustrates the convergence behavior of cases IV(a) and IV(b). Figure 9(*c*) shows that the hybrid scheme convergence behavior was oscillatory. The erratic behavior shown by the results of Figure 9(*d*) can probably be attributed to the accumulation of small round-off errors.

The numerical solutions obtained from the different approaches described above were compared to each other in order to assess the accuracy and the consistency of the solutions obtained. Figure 10 shows the plots of the solutions using the upwinding, central differencing (or hybrid), and semi-analytical solutions for cases I–IV. It is evident from these plots that the solutions from the central differencing (or hybrid) and semianalytical methods were very similar in all four cases. However, Figs. 10(*c*) and 10(*d*) show that the solutions from the upwind method were slightly different from those from the other two methods for cases III and IV.

Finally, the Euler-Cauchy Eq. (A10*b*) was solved using the upwinding scheme in order to verify the code. The analytical solution given in Eq. (A11*b*) and the numerical solution were very similar. Figure 11 shows the plot of the exact error, i.e., the difference in the two solutions at $x=0.5$ for different values of grid spacing dx. It is evident from the figure that the difference between the two solutions was, at most, on the order of 10^{-3}.

References

[1] Richardson, L. F., 1910, "The Approximate Arithmetical Solution by Finite Differences of Physical Problems Involving Differential Equations, With an Application to the Stresses In a Masonry Dam," Philos. Trans. R. Soc. London, Ser. A **210**, pp. 307–357.

[2] Richardson, L. F., and Gaunt, J. A., 1927, "The Deferred Approach to the Limit," Philos. Trans. R. Soc. London, Ser. A **226**, pp. 299–361.

[3] Celik, I., Chen, C. J., Roache, P. J., and Scheurer, G., eds., 1993, "Quantification of Uncertainty in Computational Fluid Dynamics," *ASME Fluids Engineering Div. Summer Meeting*, 158, Washington, DC, June 20-24.

[4] Roache, P. J., 1993, "A Method for Uniform Reporting of Grid Refinement Studies," *Proc. of Symp. on Quantification of Uncertainty in Computational Fluid Dynamics*, ASME, New York, I. Celik et al., eds., *ASME Fluids Engineering Div. Summer Meeting*, 158, Washington DC, June 20-24, pp. 109–120.

[5] Roache, P. J., 1998, *Verification and Validation in Computational Science and Engineering*, Hermosa Publishers, Albuquerque.

[6] Celik, I., and Zhang, W. M, 1993, "Application of Richardson Extrapolation to Some Simple Turbulent Flow Calculations," *Proc. of Symp. on Quantification of Uncertainty in Computational Fluid Dynamics*, ASME, New York, I. Celik et al., eds., *ASME Fluids Engineering Div. Summer Meeting*, 158, Washington, DC, June 20–24, pp. 29–38.

[7] Celik, I., and Karatekin, O., 1997, "Numerical Experiments on Application of Richardson Extrapolation With Nonuniform Grids," ASME J. Fluids Eng. **119**, pp. 584–590.

[8] Stern, F., Wilson, R. V., Coleman, H. W., and Paterson, E. G., 2001, "Comprehensive Approach to Verification and Validation of CFD Simulations: Part 1. Methodology and Procedures," ASME J. Fluids Eng. **123**, pp. 793–802.

[9] Cadafalch, J., Perez-Segarra, C. D., Consul, R., and Oliva, A., 2002, "Verification of Finite Volume Computations on Steady-State Fluid Flow and Heat Transfer," ASME J. Fluids Eng. **124**, pp. 11–21.

[10] Eca, L., and Hoekstra, M., 2002, "An Evaluation of Verification Procedures for CFD Applications," *24th Symp. on Naval Hydrodynamics*, Fukuoka, Japan, July 8–13.

[11] Celik, I., and Li, J., 2004, "Assessment of Numerical Uncertainty for the Calculations of Turbulent Flow over a Backward Facing Step," *Workshop on Uncertainty Estimation*, Lisbon, Oct. 21–22.

[12] Roy, C. J., 2003, private communication.

[13] Klein, M., 2004, private communication.

[14] Fox, L., 1957, *The Numerical Solution of Two-point Boundary Value Problems in ODE's*, Clarendon Press, Oxford, pp. 332.

[15] Phillips, G. M., and Taylor, P. J., 1973, *Theory and Applications of Numerical Analysis*, Academic Press, New York, pp. 345.